1392 *Inorg. Chem.* **2011**, *50*, 1392–1401
DOI: 10.1021/ic102057p

Inorganic Chemistry
Article

Structure and Gas Sorption Behavior of a New Three Dimensional Porous Magnesium Formate

Arijit Mallick, Subhadeep Saha, Pradip Pachfule, Sudip Roy, and Rahul Banerjee*

Physical/Materials Chemistry Division, National Chemical Laboratory, Dr. Homi Bhabha Road, Pune-411008, India

Received October 12, 2010

A new three-dimensional magnesium formate polymorph, namely, γ-$[Mg_3(O_2CH)_6]$ has been synthesized via in situ formate anion generation method. γ-Mg-formate crystallizes in space group *Pbcn*, and structural determination by X-ray single crystal diffraction reveals a three-dimensional network of Mg^{2+} linked by formate anions. All formate anions possess similar binding mode to the metal center with one oxygen of a particular formate anion binds to one metal center (μ^1 oxygen) and other oxygen binds to two metal centers (μ^2 oxygen). N_2 adsorption studies indicate that the framework displays permanent porosity. The specific surface area of γ-Mg-formate (BET, 120 m^2 gm^{-1}) is lower than the α- polymorph (BET, 150 m^2 gm^{-1}). However, the initial hydrogen uptake of γ-Mg-formate reached almost 1.0 wt % when the adsorbate pressure approached 760 Torr at 77 K. This is higher than the hydrogen uptake of α-Mg-formate (0.6 wt %). γ-Mg-formate, shows a moderate affinity and capacity for CO_2 (3.4 Å kinetic diameter) at 298 K. The CO_2 uptake at 760 Torr is 2.01 mmol gm^{-1}(47.0 cc gm^{-1}). Although this CO_2 uptake is somewhat modest, it compares well with the CO_2 uptake of several Mg-MOFs and ZIFs reported in the literature.

Introduction

Metal−organic frameworks (MOFs)[1] represent a new class of network solids that have great potential in applications like separation,[2] storage[3] and controlled drug delivery.[4] Recently, the research on porous metal formates, a sub family of MOFs, has emerged as one of the most active areas of research because of their potential applications as adsorbents,[5] heterogeneous catalysis[6] and in multiferroics.[7] Although molecular formates are well-known in literature,[8] but a challenging target in this field is the design and synthesis of extra-large microporous formate frameworks so that catalysis and separation can be performed on large molecules. To achieve high porosity with large pore openings, several

*To whom correspondence should be addressed. E-mail: r.banerjee@ncl.res.in. Fax: + 91-20-25902636. Phone: + 91-20-25902535.

(1) (a) Allendorf, M. D.; Bauer, C. A.; Bhakta, R. K.; Houk, R. J. T. *Chem. Soc. Rev.* **2009**, *38*, 1330. (b) Chen, B.; Xiang, S.; Qian, G. *Acc. Chem. Res.* **2010**, *43*, 1115. (c) Czaja, A. U.; Trukhan, N.; Muller, U. *Chem. Soc. Rev.* **2009**, *38*, 1284. (d) Eddaoudi, M.; Moler, D. B.; Li, H.; Chen, B.; Reineke, T. M.; O'Keeffe, M.; Yaghi, O. M. *Acc. Chem. Res.* **2001**, *34*, 319. (e) Evans, O. R.; Lin, W. *Acc. Chem. Res.* **2002**, *35*, 511. (f) Farha, O. K.; Hupp, J. T. *Acc. Chem. Res.* **2010**, *43*, 1166. (g) Ferey, G.; Serre, C. *Chem. Soc. Rev.* **2009**, *38*, 1380. (h) Hill, R. J.; Long, D.-L.; Champness, N. R.; Hubberstey, P.; Schröder, M. *Acc. Chem. Res.* **2005**, *38*, 335. (i) Iv, J. J. P.; Perman, J. A.; Zaworotko, M. J. *Chem. Soc. Rev.* **2009**, *38*, 1400. (j) Kurmoo, M. *Chem. Soc. Rev.* **2009**, *38*, 1353. (k) Lee, J.; Farha, O. K.; Roberts, J.; Scheidt, K. A.; Nguyen, S. T.; Hupp, J. T. *Chem. Soc. Rev.* **2009**, *38*, 1450. (l) MacGillivray, L. R.; Papaefstathiou, G. S.; Friščić, T.; Hamilton, T. D.; Bučar, D.-K.; Chu, Q.; Varshney, D. B.; Georgiev, I. G. *Acc. Chem. Res.* **2008**, *41*, 280. (m) Murray, L. J.; Dinca, M.; Long, J. R. *Chem. Soc. Rev.* **2009**, *38*, 1294. (n) Ockwig, N. W.; Delgado-Friedrichs, O.; O'Keeffe, M.; Yaghi, O. M. *Acc. Chem. Res.* **2005**, *38*, 176. (o) Parnham, E. R.; Morris, R. E. *Acc. Chem. Res.* **2007**, *40*, 1005. (p) Phan, A.; Doonan, C. J.; Uribe-Romo, F. J.; Knobler, C. B.; O'Keeffe, M.; Yaghi, O. M. *Acc. Chem. Res.* **2009**, *43*, 58. (q) Tranchemontagne, D. J.; Mendoza-Cortes, J. L.; O'Keeffe, M.; Yaghi, O. M. *Chem. Soc. Rev.* **2009**, *38*, 1257. (r) Wang, Z.; Cohen, S. M. *Chem. Soc. Rev.* **2009**, *38*, 1315. (s) Yaghi, O. M.; Li, H.; Davis, C.; Richardson, D.; Groy, T. L. *Acc. Chem. Res.* **1998**, *31*, 474. (t) Yu, J.; Xu, R. *Acc. Chem. Res.* **2010**, *43*, 1195. (u) Zacher, D.; Shekhah, O.; Woll, C.; Fischer, R. A. *Chem. Soc. Rev.* **2009**, *38*, 1418.

(2) (a) Bárcia, P. S.; Zapata, F.; Silva, J. A. C.; Rodrigues, A. E.; Chen, B. *J. Phys. Chem. B* **2007**, *111*, 6101. (b) Chen, B.; Ma, S.; Hurtado, E. J.; Lobkovsky, E. B.; Zhou, H.-C. *Inorg. Chem.* **2007**, *46*, 8490. (c) Chen, B.; Ma, S.; Zapata, F.; Fronczek, F. R.; Lobkovsky, E. B.; Zhou, H.-C. *Inorg. Chem.* **2007**, *46*, 1233. (d) Gu, Z.-Y.; Jiang, D.-Q.; Wang, H.-F.; Cui, X.-Y.; Yan, X.-P. *J. Phys. Chem. C* **2009**, *114*, 311. (e) Kim, H.; Kim, Y.; Yoon, M.; Lim, S.; Park, S. M.; Seo, G.; Kim, K. *J. Am. Chem. Soc.* **2010**, *132*, 12200. (f) Zhong, D.-C.; Lu, W.-G.; Jiang, L.; Feng, X.-L.; Lu, T.-B. *Cryst. Growth Des.* **2009**, *10*, 739.

(3) (a) An, J.; Fiorella, R. P.; Geib, S. J.; Rosi, N. L. *J. Am. Chem. Soc.* **2009**, *131*, 8401. (b) Belof, J. L.; Stern, A. C.; Eddaoudi, M.; Space, B. *J. Am. Chem. Soc.* **2007**, *129*, 15202. (c) Chen, B.; Ma, S.; Zapata, F.; Lobkovsky, E. B.; Yang, J. *Inorg. Chem.* **2006**, *45*, 5718. (d) Eddaoudi, M.; Li, H.; Yaghi, O. M. *J. Am. Chem. Soc.* **2000**, *122*, 1391. (e) Farha, O. K.; Malliakas, C. D.; Kanatzidis, M. G.; Hupp, J. T. *J. Am. Chem. Soc.* **2009**, *132*, 950. (f) Luo, J.; Xu, H.; Liu, Y.; Zhao, Y.; Daemen, L. L.; Brown, C.; Timofeeva, T. V.; Ma, S.; Zhou, H.-C. *J. Am. Chem. Soc.* **2008**, *130*, 9626. (g) Ma, S.; Sun, D.; Ambrogio, M.; Fillinger, J. A.; Parkin, S.; Zhou, H.-C. *J. Am. Chem. Soc.* **2007**, *129*, 1858. (h) Mulfort, K. L.; Hupp, J. T. *J. Am. Chem. Soc.* **2007**, *129*, 9604. (i) Sava, D. F.; Kravtsov, V. C.; Eckert, J.; Eubank, J. F.; Nouar, F.; Eddaoudi, M. *J. Am. Chem. Soc.* **2009**, *131*, 10394. (j) Thornton, A. W.; Nairn, K. M.; Hill, J. M.; Hill, A. J.; Hill, M. R. *J. Am. Chem. Soc.* **2009**, *131*, 10662. (k) Jin, P.; Dalgarno, S. J.; Barnes, C.; Teat, S. J.; Atwood, J. L. *J. Am. Chem. Soc.* **2008**, *130*, 17262. (l) McKinlay, R. M.; Thallapally, P. K.; Atwood, J. L. *Chem. Commun.* **2006**, 2956. (m) Heaven, M. W.; Cave, G. W. V.; McKinlay, R. M.; Antesberger, J.; Dalgarno, S. J.; Thallapally, P. K.; Atwood, J. L. *Angew. Chem., Int. Ed.* **2006**, *45*, 6221. (n) McKinlay, R. M.; Atwood, J. L. *Angew. Chem., Int. Ed.* **2007**, *46*, 2394.

Published on Web 12/30/2010

approaches have been explored in the past few years. In particular, a number of porous formates have been synthesized in the presence of organic amines as structure-directing agents (SDA).[9] The use of organic amines, a well-known SDA for zeolite synthesis,[10] is currently receiving great attention because change in the SDA may result three-dimensional (3D) porous metal-formates with different architecture and diverse porosity.

Although MOFs containing transition metals (e.g., cobalt, nickel, zinc, and copper) have been widely investigated,[11] the coordination chemistry of MOFs based on main-group metals, in particular, light main group metals (like Mg^{2+} or Ca^{2+}) are very rare.[12] Divalent magnesium has a number of similarities to the transition metal ions as it prefers octahedral coordination, has a comparable ionic radius (72 pm for Mg^{2+} compared to 74 pm for Zn^{2+} and 73 pm for Cu^{2+}) and similar hydration energy. However, only a handful of magnesium containing MOFs are reported, as magnesium carboxylates rarely form extended 3D structures because Mg^{2+} has a high affinity for oxygen donor atoms of water and other polar solvents.[13] Recent research on Mg-based MOFs showed that some Mg-MOF has the capability to store significant amount of carbon dioxide (8.08 mmol/g at 298 K) and hydrogen (1.96 wt % at 77 K).[14] However, often it has been found that the competitive coordination by water or other solvents with the polyfunctional ligands used for the synthesis of Mg-MOFs, makes it more challenging to get a 3D Mg-MOF with high porosity.

We report here synthesis and structural studies of new 3D magnesium formate polymorph, namely, γ-$[Mg_3(O_2CH)_6]$ synthesized via in situ formate anion generation method and adding 1,3-benzene-ditetrazole as SDA.[15] The crystal structure of this new γ- polymorph of magnesium formate is completely different from other reported magnesium formates (α and β polymorph).[16] The occurrence of polymorphism[17] is likely for a particular compound that can be synthesized or crystallized under different experimental conditions. The structure of γ-$[Mg_3(O_2CH)_6]$ has been determined by single crystal X-ray diffraction (XRD) and further identified by IR spectroscopy (FTIR) and powder X-ray diffraction (PXRD). We measured the thermal stability of these γ-$[Mg_3(O_2CH)_6]$ by thermogravimetric analysis (TGA) and its ability to

(4) (a) Dupuis, A.; Guo, N.; Gao, Y.; Godbout, N.; Lacroix, S.; Dubois, C.; Skorobogatiy, M. *Opt. Lett.* **2007**, *32*, 109. (b) Hinks, N. J.; McKinlay, A. C.; Xiao, B.; Wheatley, P. S.; Morris, R. E. *Microporous Mesoporous Mater.* **2010**, *129*, 330. (c) Horcajada, P.; Serre, C.; Maurin, G.; Ramsahye, N. A.; Balas, F.; Vallet-Regí, M. a.; Sebban, M.; Taulelle, F.; Férey, G. r. *J. Am. Chem. Soc.* **2008**, *130*, 6774. (d) Lin, W.; Rieter, W.; Taylor, K. *Angew. Chem., Int. Ed.* **2009**, *48*, 650. (e) Shekhah, O.; Wang, H.; Paradinas, M.; Ocal, C.; Schupbach, B.; Terfort, A.; Zacher, D.; Fischer, R. A.; Woll, C. *Nat. Mater.* **2009**, *8*, 481. (f) Taylor-Pashow, K. M. L.; Rocca, J. D.; Xie, Z.; Tran, S.; Lin, W. *J. Am. Chem. Soc.* **2009**, *131*, 14261. (g) Vallet-Regí, M.; Balas, F.; Arcos, D. *Angew. Chem., Int. Ed.* **2007**, *46*, 7548.

(5) (a) Dybtsev, D. N.; Chun, H.; Yoon, S. H.; Kim, D.; Kim, K. *J. Am. Chem. Soc.* **2003**, *126*, 32. (b) Kim, H.; Samsonenko, D. G.; Yoon, M.; Yoon, J. W.; Hwang, Y. K.; Chang, J.-S.; Kim, K. *Chem. Commun.* **2008**, 4697. (c) Li, K.; Olson, D. H.; Lee, J. Y.; Bi, W.; Wu, K.; Yuen, T.; Xu, Q.; Li, J. *Adv. Funct. Mater.* **2008**, *18*, 2205. (d) Wang, Z.; Zhang, B.; Kurmoo, M.; Green, M. A.; Fujiwara, H.; Otsuka, T.; Kobayashi, H. *Inorg. Chem.* **2005**, *44*, 1230. (e) Wang, Z. M.; Zhang, Y. J.; Liu, T.; Kurmoo, M.; Gao, S. *Adv. Funct. Mater.* **2007**, *17*, 1523.

(6) (a) Chizallet, C. l.; Lazare, S.; Bazer-Bachi, D.; Bonnier, F.; Lecocq, V.; Soyer, E.; Quoineaud, A.-A.; Bats, N. *J. Am. Chem. Soc.* **2010**, *132*, 12365. (b) Cho, S.-H.; Ma, B.; Nguyen, S. T.; Hupp, J. T.; Albrecht-Schmitt, T. E. *Chem. Commun.* **2006**, 2563. (c) Dybtsev, D. N.; Nuzhdin, A. L.; Chun, H.; Bryliakov, K. P.; Talsi, E. P.; Fedin, V. P.; Kim, K. *Angew. Chem., Int. Ed.* **2006**, *45*, 916. (d) Hoskins, B. F.; Robson, R. *J. Am. Chem. Soc.* **1990**, *112*, 1546. (e) Hwang, Y.; Hong, D. Y.; Chang, J. S.; Jhung, S.; Seo, Y. K.; Kim, J.; Vimont, A.; Daturi, M.; Serre, C.; Férey, G. *Angew. Chem., Int. Ed.* **2008**, *120*, 4212. (f) Tanabe, K. K.; Cohen, S. M. *Inorg. Chem.* **2010**, *49*, 6766. (g) Wu, C. D.; Lin, W. *Angew. Chem., Int. Ed.* **2007**, *46*, 1075. (h) Wu, C.-D.; Hu, A.; Zhang, L.; Lin, W. *J. Am. Chem. Soc.* **2005**, *127*, 8940.

(7) (a) Pointillart, F.; Cauchy, T.; Le Gal, Y.; Golhen, S.; Cador, O.; Ouahab, L. *Chem. Commun.* **2010**, *46*, 4947. (b) Rogez, G.; Viart, N.; Drillon, M. *Angew. Chem., Int. Ed.* **2010**, *49*, 1921.

(8) (a) Casellato, U.; Vigato, P. A.; Vidali, M. *Coord. Chem. Rev.* **1978**, *26*, 85. (b) Honkonen, R. S.; Ellis, P. D. *J. Am. Chem. Soc.* **1984**, *106*, 5488. (c) Kiriyama, H. I. a. K. M., R. *Acta Crystallogr.* **1954**, *7*, 482. (d) Wilson, M. P.; Alcock, N. W.; Rodger, P. M. *Inorg. Chem.* **2006**, *45*, 4359. (e) Viertelhaus, M.; Adler, P.; Clérac, R.; Anson, C.; Powell, A. *Eur. J. Inorg. Chem.* **2005**, *2005*, 692. (f) Kiriyama, R.; Ibamoto, H.; Matsuo, K. *Acta Crystallogr.* **1954**, *7*, 482. (g) Habeeb, J. J.; Tuck, D. G. *Dalton Trans.* **1973**, *3*, 243. (h) Casellato, U.; Vigato, P.; Vidali, M. *Coord. Chem. Rev.* **1978**, *26*, 285. (i) Honkonen, R. S.; Ellis, P. D. *J. Am. Chem. Soc.* **1984**, *106*, 5488. (j) Arii, T.; Kishi, A. *Thermochim. Acta* **1999**, *325*, 157. (k) Wilson, M. P.; Alcock, N. W.; Rodger, P. M. *Inorg. Chem.* **2006**, *45*, 4539.

(9) (a) He, J.; Zhang, Y.; Pan, Q.; Yu, J.; Ding, H.; Xu, R. *Microporous Mesoporous Mater.* **2006**, *90*, 145. (b) Wang, Z.; Zhang, B.; Fujiwara, H.; Kobayashi, H.; Kurmoo, M. *Chem. Commun.* **2004**, 416. (c) Wang, Z.; Zhang, X.; Batten, S. R.; Kurmoo, M.; Gao, S. *Inorg. Chem.* **2007**, *46*, 8439.

(10) (a) Han, B.; Lee, S.-H.; Shin, C.-H.; Cox, P. A.; Hong, S. B. *Chem. Mater.* **2005**, *17*, 477. (b) Lee, H.; Zones, S. I.; Davis, M. E. *Nature* **2003**, *425*, 385. (c) Tagliabue, M.; Carluccio, L. C.; Ghisletti, D.; Perego, C. *Catal. Today* **2003**, *81*, 405. (d) Wagner, P.; Nakagawa, Y.; Lee, G. S.; Davis, M. E.; Elomari, S.; Medrud, R. C.; Zones, S. I. *J. Am. Chem. Soc.* **1999**, *122*, 263.

(11) (a) Banerjee, R.; Phan, A.; Wang, B.; Knobler, C.; Furukawa, H.; O'Keeffe, M.; Yaghi, O. M. *Science* **2008**, *319*, 939. (b) Greathouse, J. A.; Allendorf, M. D. *J. Phys. Chem. C* **2008**, *112*, 5795. (c) Huang, X. C.; Lin, Y. Y.; Zhang, J. P.; Chen, X. M. *Angew. Chem., Int. Ed.* **2006**, *118*, 1587. (d) Livage, C.; Egger, C.; Ferey, G. *Chem. Mater.* **1999**, *11*, 1546. (e) Livage, C.; Egger, C.; Férey, G. *Chem. Mater.* **2001**, *13*, 410. (f) Livage, C.; Guillou, N.; Chaigneau, J.; Rabu, P.; Drillon, M.; Férey, G. *Angew. Chem., Int. Ed.* **2005**, *44*, 6488. (g) Lu, Y.; Tonigold, M.; Bredenkötter, B.; Volkmer, D.; Hitzbleck, J.; Langstein, G. *Z. Anorg. Allg. Chem.* **2008**, *634*, 2411. (h) Pachfule, P.; Das, R.; Poddar, P.; Banerjee, R. *Cryst. Growth Des.* **2010**, *10*, 2475. (i) Pachfule, P.; Dey, C.; Panda, T.; Banerjee, R. *CrystEngComm* **2010**, *12*, 1600.

(12) (a) Abrahams, B. F.; Hawley, A.; Haywood, M. G.; Hudson, T. A.; Robson, R.; Slizys, D. A. *J. Am. Chem. Soc.* **2004**, *126*, 2894. (b) Cheon, Y. E.; Park, J.; Suh, M. P. *Chem. Commun.* **2009**, 5436. (c) Davies, R. P.; Less, R. J.; Lickiss, P. D.; White, A. J. P. *Dalton Trans.* **2007**, 2528. (d) Dietzel, P. D. C.; Blom, R.; Fjellvåg, H. *Eur. J. Inorg. Chem.* **2008**, *2008*, 3624. (e) Falcão, E. H. L.; Naraso; Feller, R. K.; Wu, G.; Wudl, F.; Cheetham, A. K. *Inorg. Chem.* **2008**, *47*, 8336. (f) Guo, Z.; Li, G.; Zhou, L.; Su, S.; Lei, Y.; Dang, S.; Zhang, H. *Inorg. Chem.* **2009**, *48*, 8069. (g) Gurunatha, K. L.; Uemura, K.; Maji, T. K. *Inorg. Chem.* **2008**, *47*, 6578. (h) Hamilton, B. H.; Kelly, K. A.; Malasi, W.; Ziegler, C. J. *Inorg. Chem.* **2003**, *42*, 3067. (i) Jokiniemi, J.; Vuokila-Laine, E.; Peraniemi, S.; Vepsalainen, J. J.; Ahlgren, M. *CrystEngComm* **2007**, *9*, 158. (j) Kam, K. C.; Young, K. L. M.; Cheetham, A. K. *Cryst. Growth Des.* **2007**, *7*, 1522. (k) Ma, S.; Fillinger, J. A.; Ambrogio, M. W.; Zuo, J.-L.; Zhou, H.-C. *Inorg. Chem. Commun.* **2007**, *10*, 220. (l) Senkovska, I.; Fritsch, J.; Kaskel, S. *Eur. J. Inorg. Chem.* **2007**, *2007*, 5475. (m) Senkovska, I.; Kaskel, S. *Eur. J. Inorg. Chem.* **2006**, *2006*, 4564. (n) Tobbens, D. M.; Hummel, M.; Kaindl, R.; Schottenberger, H.; Kahlenberg, V. *CrystEngComm* **2008**, *10*, 327. (o) Volkringer, C.; Loiseau, T.; Marrot, J.; Ferey, G. *CrystEngComm* **2009**, *11*, 58. (p) Williams, C. A.; Blake, A. J.; Wilson, C.; Hubberstey, P.; Schröder, M. *Cryst. Growth Des.* **2008**, *8*, 911. (q) Xiao, D. R.; Wang, E. B.; An, H. Y.; Su, Z. M.; Li, Y. G.; Gao, L.; Sun, C. Y.; Xu, L. *Chem. Eur. J.* **2005**, *11*, 6673. (r) Zhou, W.; Wu, H.; Yildirim, T. *J. Am. Chem. Soc.* **2008**, *130*, 15268. (s) Mallick, A.; Saha, S.; Pachfule, P.; Roy, S.; Banerjee, R. *J. Mater. Chem.* **2010**, *20*, 9073.

(13) (a) Dincă, M.; Long, J. R. *J. Am. Chem. Soc.* **2005**, *127*, 9376. (b) Samsonenko, D.; Kim, H.; Sun, Y.; Kim, G. H.; Lee, H. S.; Kim, K. *Chem. Asian J.* **2007**, *2*, 484. (c) Zhang, J.; Chen, S.; Valle, H.; Wong, M.; Austria, C.; Cruz, M.; Bu, X. *J. Am. Chem. Soc.* **2007**, *129*, 14168.

(14) (a) Britt, D.; Furukawa, H.; Wang, B.; Glover, T. G.; Yaghi, O. M. *Proc. Natl. Acad. Sci. U.S.A.* **2009**, *106*, 20637. (b) Caskey, S. R.; Wong-Foy, A. G.; Matzger, A. J. *J. Am. Chem. Soc.* **2008**, *130*, 10870. (c) Rowsell, J. L. C.; Yaghi, O. M. *J. Am. Chem. Soc.* **2006**, *128*, 1304.

(15) Massi, M.; Ogden, M. I.; Radomirovic, T.; Jones, F. *CrystEngComm*, **2010**, *12*, 4205.

(16) (a) Viertelhaus, M.; Anson, C. E.; Powell, A. K. *Z. Anorg. Allg. Chem.* **2005**, *631*, 2365. (b) Rood, J. A.; Noll, B. C.; Henderson, K. W. *Inorg. Chem.* **2006**, *45*, 5521. (c) Schmitz, B.; Krkljus, I.; Leung, E.; Höffken, H.; Müller, U.; Hirscher, M. *ChemSusChem.* **2010**, *3*, 758.

adsorb and release carbon dioxide (CO_2) and hydrogen (H_2) gas. In addition, in situ variable temperature PXRD has been carried out on α and γ magnesium formate to analyze their stability and crystallinity at high temperature and dehydration−rehydration cycle. We have used Grand Canonical Monte Carlo (GCMC) simulation[18] to predict the initial positions of the hydrogen molecules in the framework and Density Functional Theory (DFT) method to optimize the positions of the each hydrogen molecules in the framework and their related adsorption energies.

Experimental Section

General Procedures. All reagents and solvents for synthesis and analysis were commercially available and used as received. The Fourier transform (FT) IR spectra (KBr pellet) were taken on Perkin Elmer FT-IR Spectrum (Nicolet) spectrometer. PXRD patterns were recorded on a Phillips PANalytical diffractometer for Cu $K\alpha_1$ radiation ($\lambda = 1.5406$ Å), with a scan speed of 2° min^{-1} and a step size of 0.02° in 2θ. Thermogravimetric experiments (TGA) were carried out in the temperature range of 25−800 °C on a SDT Q600 TG-DTA analyzer under N_2 atmosphere at a heating rate of 10 °C min^{-1}. All low pressure gas adsorption experiments (up to 760 Torr) were performed on a Quantachrome Quadrasorb automatic volumetric instrument.

Synthesis of γ-Mg-formate $Mg_3(O_2CH)_6\supset[NH(CH_3)_2]_{0.5}$. As 1,3-benzene-ditetrazole is sparingly soluble in water at moderate temperature, we used the solvent DMF in which it is readily soluble. We used the solvothermal condition (Teflon-lined stainless steel autoclave at 125 to 150 °C) for synthesis which results in the formation of single crystals suitable for X-ray diffraction. Before solvothermal reactions, stirring of the heterogeneous solutions for a period 30 min was helpful for the high purity of the product. Solvothermal reaction of $Mg(CO_2CH_3)_2\cdot 4H_2O$ (0.214 g, 1 mmol) with 1,3-benzene-ditetrazole (0.214 g, 1 mmol) in a 25 mL Teflon-lined stainless steel autoclave in 5 mL of dimethylformamide (DMF) and 0.2 mL of HNO_3 (3.6 M) mixture at 150 °C for 60 h produces colorless crystals of $Mg_3(O_2CH)_6\supset[NH(CH_3)_2]_{0.5}$ in 61% yield. Crystals were collected by filtration and dried in air (10 min). [Yield: 61%, 0.130 g depending on $Mg(CO_2CH_3)_2\cdot 4H_2O$]. FT-IR: (KBr 4000−400 cm^{-1}): 3302(br), 2906(w), 1683(w), 1598(s), 1404(m), 1375(m), 1364(m), 841(w), 761(w), 694(w), 574(w). Elemental Analysis Calc: C (23.20%), H (0.82%), N (1.93%); Found C (21.20%), H (0.72%), N (2.03%).

X-ray Crystallography. Single crystal data of γ-Mg-formate was collected on a Bruker SMART APEX three circle diffractometer equipped with a CCD area detector (Bruker Systems Inc., 1999a) and operated at 1500 W power (50 kV, 30 mA) to generate Mo Kα radiation ($\lambda = 0.71073$ Å). The incident X-ray beam was focused and monochromated using Bruker Excalibur Gobel mirror optics. Crystal of the γ-Mg-formate reported in the paper was mounted on nylon CryoLoops (Hampton Research) with Paratone-N (Hampton Research). Data was integrated using Bruker SAINT software.[19] Data was subsequently corrected for absorption by the program SADABS.[20] Space group determinations and tests for merohedral twinning were carried out using XPREP.[21] Here, the highest possible space group was chosen. This structure was solved by direct methods and refined using the SHELXTL 97 software suite.[22] Atoms were located from iterative examination of difference F-maps following least-squares refinements of the earlier models.[23] Hydrogen atoms were placed in calculated positions and included as riding atoms with isotropic displacement parameters 1.2−1.5 times U_{eq} of the attached C atoms. Data was collected at 293(2) K for the γ-Mg-formate reported in this paper. The structure was examined using the *Addsym* subroutine of PLATON[24] to ensure that no additional symmetry could be applied to the models. All ellipsoids in ORTEP diagrams are displayed at the 50% probability level unless noted otherwise. The Supporting Information contains a detailed data collection strategy and crystallographic data for the γ-Mg-formate reported in this paper. Crystallographic data (excluding structure factors) for the structures are reported in this paper have been deposited with the CCDC as deposition No. CCDC-791926. Copies of the data can be obtained, free of charge, on application to the CCDC, 12 Union Road, Cambridge CB2 lEZ, U.K. [fax: + 44 (1223) 336 033; e-mail: deposit@ccdc.cam.ac.uk].

N_2, H_2, and CO_2 Adsorption Measurements. Hydrogen adsorption−desorption experiments were conducted at 77 K using Quantachrome Quadrasorb automatic volumetric instrument. Ultrapure H_2 (99.95%) was purified further by using calcium aluminosilicate adsorbents to remove trace amounts of water and other impurities before introduction into the system. For measurements at 77 K, a standard low-temperature liquid nitrogen Dewar vessel was used. CO_2 adsorption−desorption measurements were done at room temperature (298 K). Before gas adsorption measurements, the sample was activated at room temperature (for 24 h) and 120 °C (for 6 h) under ultrahigh vacuum (10^{-8} mbar) overnight. About 75 mg of samples were loaded for gas adsorption, and the weight of each sample was recorded before and after outgassing to confirm complete removal of all guest molecules.

Computational Procedures

Initial Structure Generation. Selection of initial positions of hydrogen molecules in the framework is the most important step for calculating the probable binding sites and the corresponding binding energy. Proper scanning of pore surface is important to get the adsorption site with the lowest binding energy. It is difficult to create homogeneously distributed initial positions of hydrogen molecules in the framework due to the 3D structure of the MOF. Even if we find homogeneously distributed positions, executing calculations for all the initial structures leads to large number of optimization calculations. Therefore, we choose the initial structure from the output of our classical grand canonical Monte Carlo simulation, which we have performed for calculating adsorption isotherms.

The conventional GCMC simulation technique is used to compute adsorption isotherms. The input for the simulation consists of models (structures) for the adsorbent and the adsorbate as well as force fields which describe the interactions between them. MOFs are crystalline therefore the model for the adsorbent in the atomistic representation of the framework is taken from its crystallographic coordinates. Here, for γ-Mg-formate we have

(17) (a) Desiraju, G. R. *Organic Solid State Chemistry*; Elsevier: Amsterdam, The Netherlands, 1987. (b) Desiraju, G. R. *Crystal Engineering: The Design of Organic Solids*; Elsevier: Amsterdam, The Netherlands, 1989. (c) Braga, D.; Grepioni, F. *Acc. Chem. Res.* **2000**, *33*, 601. (d) Braga, D.; Grepioni, F.; Desiraju, G. R. *Chem. Rev.* **1998**, *98*, 1375. (e) Davey, R. J.; Blagden, N.; Righini, S.; Alison, H.; Quayle, M. J.; Fuller, S. *Cryst. Growth Des.* **2000**, *1*, 59. (f) Moulton, B.; Zaworotko, M. J. *Chem. Rev.* **2001**, *101*, 1629. (g) Weissbuch, I.; Torbeev, V. Y.; Leiserowitz, L.; Lahav, M. *Angew. Chem., Int. Ed.* **2005**, *117*, 3290. (h) Weissbuch, I.; Zbaida, D.; Addadi, L.; Leiserowitz, L.; Lahav, M. *J. Am. Chem. Soc.* **1987**, *109*, 1869.

(18) Frenkel, D.; Smit, B.; *Understanding Molecular Simulation*, 2nd ed.; Academic Press: San Diego, 2002.

(19) *SMART*, Version 5.05; Bruker AXS, Inc.: Madison, WI, 1998.

(20) *SAINT-Plus*, Version 7.03; Bruker AXS, Inc.: Madison, WI, 2004.

(21) Sheldrick, G. M. *SADABS* (*Version 2.03*) *and TWINABS* (*Version 1.02*); University of Göttingen: Göttingen, Germany, 2002.

(22) Sheldrick, G. M. *SHELXS '97*; University of Göttingen: Göttingen, Germany, 1997.

(23) Sheldrick, G. M. *SHELXTL '97*; University of Göttingen: Göttingen, Germany, 1997.

(24) Spek, A. L. *PLATON, A Multipurpose Crystallographic Tool,* ; Utrecht University: Utrecht, The Netherlands, 2005.

used the original crystal structure ignoring the solvent molecule residing in the pore. In all the simulations, the framework is treated as rigid (a valid assumption for many MOFs at low temperature), although models for flexible MOFs have been proposed recently.[25] We have calculated the theoretical hydrogen adsorption isotherm for γ-Mg-formate and α-Mg-formate formate. To avoid boundary or finite size effects and to allow simulations that are valid for the extended crystal lattice, periodic boundary conditions has been used,[18] resulting in simulations that take place in an infinite, perfect structure. To model adsorbate/adsorbate and adsorbate/framework interactions, van der Waals interactions (normally modeled by Lennard-Jones potentials) have been taken into account. Lennard-Jones (LJ) parameters for the individual atoms and for H_2 molecule UFF[26] potential parameters has been considered. LJ potential parameters for cross interactions were computed from Lorentz−Berthelot combining rules. The cutoff radii for both the MOFs were set to be 4.8 Å. For GCMC calculations the volume (V), the temperature (T), and the chemical potential (μ) are kept fixed, and under these conditions, the average number of H_2 molecules adsorbed is computed. Each step in the Monte Carlo routine consisted of the insertion of a new molecule, deletion of an existing molecule, or translation of an existing molecule. A total of 5 million steps were used, the first half for equilibration and the second half to calculate the ensemble averages. A configuration is defined as an attempted translation, rotation, creation, or deletion of a H_2 molecule. The probability of attempting creation or deletion of a molecule was set to 0.3; an equation of state for hydrogen[27] was used to obtain the relationship between the bulk pressure and fugacity. We have converted the total adsorption obtained from simulation to excess adsorption to compare with the experiments. The details of the conversion calculations can be found in the literature. Along with the adsorption isotherm, the positions (coordinates) of the adsorbed hydrogen molecules in the pores of both of α and γ-Mg-formate were obtained. Finite structures (shown in Supporting Information, Figure S8) of the frameworks have been generated with different positions of hydrogen molecules. These initial structures were further optimized by ab initio quantum chemical calculations.

Calculation of Adsorption Energy and Site. Finite structure obtained from the periodic structure possesses artificial dangling bonds. We have saturated those bonds with H atoms. For geometry optimization, the Gaussian 09 software suite[28] has been used. The ModRedundant option has been employed to perform the selective optimization of H atoms which have been attached to the clusters to saturate the dangling bonds at the B3LYP[29]/6-31G level of theory to get the energy, $E_{(\mathrm{BAREMOF})}$ of the finite structure. A hydrogen molecule on the finite structure was inserted at the same positions that we obtained from GCMC simulation. Then we have optimized the positions of hydrogen molecules of each initial structure containing finite formate clusters (α-formate and γ-formate both) and one hydrogen molecule using DFT with a 6-31G basis set. The energies we calculated from these calculations are for adsorbate−adsorbent complex, $E_{(\mathrm{BAREMOF+H2})}$. We have determined the binding energy of hydrogen using the following equation, where $E_{(\mathrm{H2})}$ is the energy of H_2 molecule obtained from DFT calculation with the same basis set.

$$E_{\mathrm{ads}} = E_{(\mathrm{BAREMOF+H2})} - (E_{(\mathrm{BAREMOF})} + E_{(\mathrm{H2})})$$

Adsorption energies after optimization of all initial configurations for each type of MOFs were compared. The lowest adsorption energies refer to the positions of the hydrogen molecules in the pores and reported in the paper.

Results and Discussion

Synthesis. In most of the literature on Mg-formates, Mg^{2+} centers are surrounded by formate groups as well as coordinated water molecules.[30] Till this date, there are only three anhydrous Mg-formates reported in the literature where Mg^{2+} centers are coordinated only with formate anions. Powell and co-worker[16a] first reported the solvothermal synthesis of two unsolvated Mg- formates (α form and β form) of which only the non-porous β-$[Mg(O_2CH)_2]$ form was structurally determined. Later Rood et al. reported the structural characterization and gas adsorption study of α-Mg-formate $[Mg_3(O_2CH)_6\supset HCO_2H]$.[16b] Recently there has been a report of a third anhydrous phase $Mg(HCOO)_2(HCOOH)\supset(CH_3)_2NH$.[31] Formic acid had been the source of formate anion in all these three cases. $Mg(NO_3)_2\cdot 6H_2O$ was the source of metal for the α and β form, whereas anhydrous $Mg(HCOO)_2(HCOOH)\supset(CH_3)_2NH$ could be prepared from $Mg(NO_3)_2\cdot 6H_2O$, $Mg(CO_2CH_3)_2\cdot 4H_2O$, and $Mg(ClO_4)_2\cdot 6H_2O$. We introduced a different synthetic route of generating formate anion in situ by addition of nitric acid (HNO_3) into the reaction media that contains *N*,*N*′-dimethylformamide (DMF) as a solvent.[32] We anticipated that reaction between nitric acid and DMF at high temperature and pressure inside a Teflon-lined stainless steel autoclave may create formate anion, which upon reaction with Mg^{2+} might result into Mg-formate. All our attempts to synthesize a new Mg-formate polymorph resulted into the production of mixtures of γ-Mg-formate (major product) and previously reported anhydrous $Mg(HCOO)_2(HCOOH)\supset(CH_3)_2NH$ (minor product). Our attempt of using diverse structure directing agents (like tetra-butyl ammonium salts) to synthesize phase pure

(25) Salles, F.; Ghoufi, A.; Maurin, G.; Bell, R.; Mellot-Draznieks, C.; Férey, G. *Angew. Chem., Int. Ed.* **2008**, *47*, 8487.
(26) Rappe, A. K.; Casewit, C. J.; Colwell, K. S.; Goddard, W. A.; Skiff, W. M. *J. Am. Chem. Soc.* **1992**, 114.
(27) Younglove, B. A. *J. Phys. Chem. Ref. Data* **1982**, *11*, 1.
(28) Frisch, M. J. T., G. W.; Schlegel, H. B.; Scuseria, G. E.; Robb, M. A.; Cheeseman, J. R.; Scalmani, G.; Barone, V.; Mennucci, B.; Petersson, G. A.; Nakatsuji, H.; Caricato, M.; Li, X.; Hratchian, H. P.; Izmaylov, A. F.; Bloino, J.; Zheng, G.; Sonnenberg, J. L.; Hada, M.; Ehara, M.; Toyota, K.; Fukuda, R.; Hasegawa, J.; Ishida, M.; Nakajima, T.; Honda, Y.; Kitao, O.; Nakai, H.; Vreven, T.; Montgomery, Jr., J. A.; Peralta, J. E.; Ogliaro, F.; Bearpark, M.; Heyd, J. J.; Brothers, E.; Kudin, K. N.; Staroverov, V. N.; Kobayashi, R.; Normand, J.; Raghavachari, K.; Rendell, A.; Burant, J. C.; Iyengar, S. S.; Tomasi, J.; Cossi, M.; Rega, N.; Millam, N. J.; Klene, M.; Knox, J. E.; Cross, J. B.; Bakken, V.; Adamo, C.; Jaramillo, J.; Gomperts, R.; Stratmann, R. E.; Yazyev, O.; Austin, A. J.; Cammi, R.; Pomelli, C.; Ochterski, J. W.; Martin, R. L.; Morokuma, K.; Zakrzewski, V. G.; Voth, G. A.; Salvador, P.; Dannenberg, J. J.; Dapprich, S.; Daniels, A. D.; Farkas, Ö.; Foresman, J. B.; Ortiz, J. V.; Cioslowski, J.; Fox, D. J. *Gaussian 09*; Gaussian, Inc.: Wallingford, CT, 2009.
(29) (a) Lee, C.; Yang, W.; Parr, R. G. *Phys. Rev. B* **1988**, *37*, 785. (b) Stephens, P. J.; Devlin, F. J.; Chabalowski, C. F.; Frisch, M. J. *J. Phys. Chem.* **1994**, *98*, 11623. (c) Vosko, S. H.; Wilk, L.; Nusair, M. *Can. J. Phys* **1980**, *58*, 1200. (d) Becke, A. D. *J. Chem. Phys.* **1993**, *98*, 5648.
(30) (a) Baggio, R.; Stoilova, D.; Garland, M. T. *J. Mol. Struct.* **2003**, *659*, 35. (b) Coke, E. N.; Boyle, T. J.; Rodriguez, M. A.; Alam, T. M. *Polyhedron* **2004**, *23*, 1739. (c) Osaki, K.; N., Y.; Watanabe, T. *J. Phys. Soc. Jpn.* **1964**, *19*, 717. (d) Malard, C.; Pezerat, H.; Herpin, P.; Toledano, P. *J. Solid State Chem.* **1982**, *41*, 67. (e) Ridwan *Jpn. J. Appl. Phys.* **1992**, *31*, 3559. (f) Stoilova, D.; Baggio, R.; Garland, M. T.; Marinova, D. *Vib. Spectrosc.* **2007**, *43*, 387. (g) Yamagata, K.; Achiwa, N.; Hashimoto, M.; Koyano, N.; Ridwan; Iwata, Y.; Shibuya, I. *Acta Crystallogr., Sect. C* **1992**, *48*, 793.
(31) Rossin, A.; Ienco, A.; Costantino, F.; Montini, T.; Di Credico, B.; Caporali, M.; Gonsalvi, L.; Fornasiero, P.; Peruzzini, M. *Cryst. Growth Des.* **2008**, *8*, 3302.
(32) Sava, D. F.; Kravtsov, V. C.; Nouar, F.; Wojtas, L.; Eubank, J. F.; Eddaoudi, M. *J. Am. Chem. Soc.* **2008**, *130*, 3768.

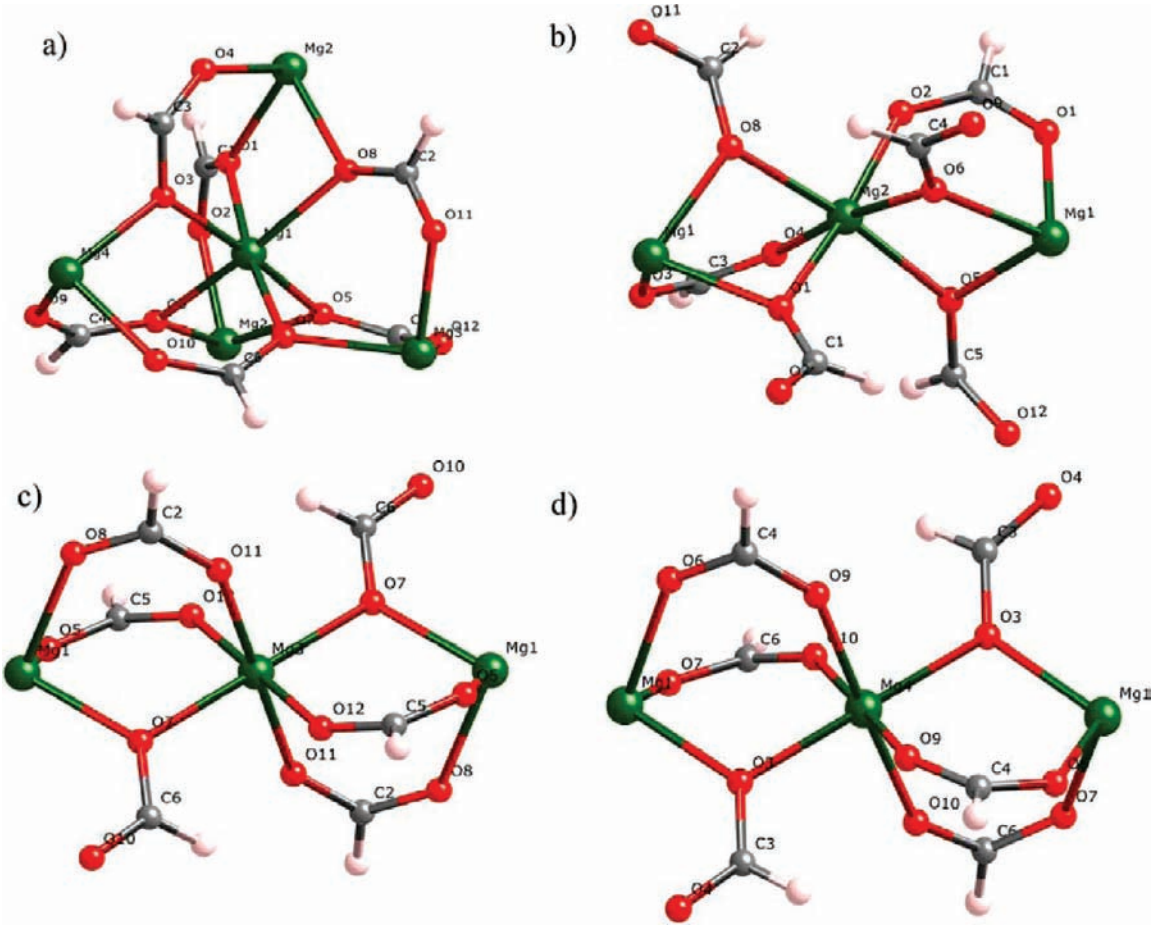

Figure 1. Local geometries surrounding the four independent, octahedrally coordinated magnesium centers within γ-Mg-formate. Color code: O (red), C (gray), Mg (green).

γ-Mg-formate also resulted in the precipitation of either the aforementioned mixtures or the unreacted starting material. However, after several attempts we discovered that solvothermal reaction (in Teflon-lined stainless steel autoclave at 125 to 150 °C) of $Mg(CO_2CH_3)_2 \cdot 4H_2O$ with nitric acid (HNO_3) in a DMF solution in the presence of 1,3-benzene-ditetrazole in 3:2:1 mol ratio for 72 h afforded a colorless homogeneous microcrystalline γ-Mg-formate as phase pure form with a dodecahedron morphology. So far we are unable to understand the role of 1,3-benzene-ditetrazole during the synthesis and crystallization of γ-Mg-formate as we are unable to find its existence in the resulting crystal structure. We anticipate that it might be acting as a structure directing agent. The as-synthesized compound is stable in most organic solvents and was characterized and formulated by single-crystal X-ray diffraction (XRD) studies as $Mg_3(O_2CH)_6 \supset [NH(CH_3)_2]_{0.5}$. The same result was obtained when we used either $Mg(ClO_4)_2 \cdot 6H_2O$ or $Mg(NO_3)_2 \cdot 6H_2O$, with no significant differences for phase purity (less than 50% yield), as confirmed by the PXRD patterns (see Supporting Information, Figure S1).

Crystal Structure of γ-Mg-formate $Mg_3(O_2CH)_6 \supset [NH(CH_3)_2]_{0.5}$. The γ-Mg-formate crystallizes in space group *Pbcn*, and structural determination by X-ray single crystal diffraction reveals a 3D network of Mg^{2+} linked by formate anions. The asymmetric unit of Mg-formate consists of four crystallographically independent Mg^{2+} ions, each of which is octahedrally coordinated by six different formate anions. All formate anions posses a similar binding mode to the metal center with one oxygen of a particular formate anion binding to one metal center (μ^1 oxygen) and the other oxygen binding to two metal centers (μ^2 oxygen). So each formate anion binds with three Mg^{2+} and each Mg^{2+} binds with six formate anions, and hence the chemical formula could be derived as $Mg_3(O_2CH)_6$ with 1:2 Mg^{2+} and ligand ratio (Figure 1). This $\eta^2\mu^3$ type binding motif is also seen in α- and β-Mg-formates. γ Mg-formate has interesting structural similarity with its α- polymorph as it contains similar coordination environments for the metal centers. Mg(1) center is connected with the six μ^2 oxygen, Mg(2) center is connected with four μ^2 oxygen and two μ^1 oxygen, whereas Mg(3) and Mg(4) centers are connected with four μ^1 oxygen and two μ^2 oxygen. Although Mg(3) and Mg(4) centers have similar connectivity but they have different coordination environments. The Mg(3) is connected to Mg(1) through two formate bridges and one μ^2 oxygen (O7), and here the bridging dihedral angles (τ)[33] are 21.29° (Mg3−O11−O8−Mg1) and 27.00° (Mg3−O1−O5−Mg1) (Figure 1c). Mg(4) is also connected with

(33) Addison, A. W.; Rao, T. N.; Reedijk, J.; Rijn, J. V.; Verschoor, G. C. *J. Chem. Soc., Dalton Trans.* **1984**, 1349.

(34) (*a*) $Mg_3(ndc)_3$/0.46 wt % of H_2; (*b*) $Mg_3(ndc)_3$/1.23 wt % of H_2; (*c*) β-$[Mg_3(O_2CH)_6]$/0.9 wt %, α-$[Mg_3(O_2CH)_6]$/0.6 wt %; (*d*) $Mg_3(ndc)_3$/ 0.78 wt % (*e*) Mg(dhtp)/ 2.00 wt % of H_2.

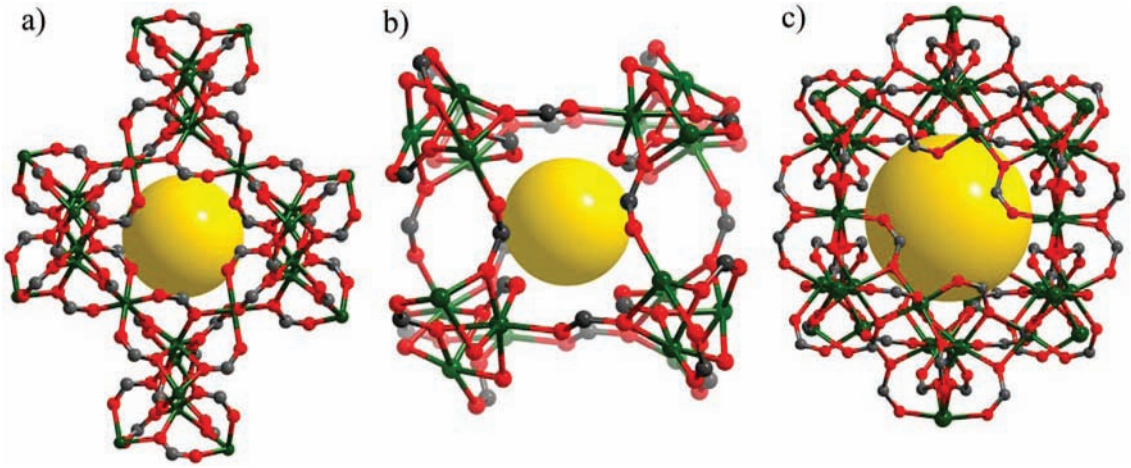

Figure 2. Ball and stick models showing packing diagram for (a) α-Mg-formate, (b) β-Mg-formate, and (c) γ-Mg-formate. Yellow balls represent the empty space inside the pores. Color code: O (red), C (gray), Mg(green).

Mg(1) through two formate bridges and one μ^2 oxygen (O3), but the dihedral bridging angles (τ) are 21.90° (Mg4−O10−O7−Mg1) and 14.18° (Mg4−O9−O6−Mg1). The Mg−O(μ^1) bond distance ranges from 2.012(2) to 2.053(3) Å, and the Mg−O(μ^2) bond distance ranges from 2.063(2) Å to 2.132(2) Å (Figure 1d). Mg(1) and Mg(2) are linked through edge-shared MgO_6 octahedra and form a one-dimensional (1D) chain along the crystallographic *a*-axis. These chains are connected to each other through vertex-sharing octahedra of Mg(3) and Mg(4), and thus it forms a 3D network. The network contains 1D channels along the crystallographic *a*-axis. Here the channels are filled by the disordered dimethylamine molecules. The void space was calculated using PLATON,[24] suggesting 5.1% void volume to the total crystal volume; however, this would be increased to 24.7% after removal of the disordered solvent molecules. The pore diameter of the channel is 3.6 Å (the channel size is measured by considering the van der Walls radii of the constituting atoms).

As mentioned previously there are three other anhydrous Mg-formates (α-Mg-formate, β-Mg-formate, $Mg(HCOO)_3 \supset (CH_3)_2NH$) reported in literature. In case of α, β and γ-Mg-formate (reported in this paper), μ^1 and μ^2 oxygen are binding with Mg^{2+} centers (Figure 2). Whereas anhydrous $Mg(HCOO)_2(HCOOH) \supset (CH_3)_2NH$ has only μ^1 oxygen binding metal centers. The α-Mg-formate crystallizes in monoclinic space group ($P2_1/n$), and β,γ-Mg-formate crystallizes in orthorhombic space group ($Pca2_1$ and $Pbcn$). All the Mg-formates contain octahedral Mg^{2+} centers. In case of α-Mg-formate and γ-Mg-formate, the edge share MgO_6 octahedra form a 1D chain, and the chains are also connected through vertex share octahedra to form 3D frame works. Whereas, in the β-Mg-formate the 1D chains, formed by edge share octahedra, are connected through formate anions (HCO_2^-) and not through vertex share octahedra. In α-Mg-formate Mg(3) and Mg(4) are in transoid orientation with respect to the planes formed by Mg(1)−Mg(2)−Mg(1) (Figure 3b) and Mg(1)−Mg(4)−Mg(1) (Figure 3c); whereas in γ-Mg-formate those Mg atoms are arranged in cisoid orientation (Figure 3e and Figure 3f). As a result, the edge shared MgO_6 octahedra in α-Mg-formate are arranged parallel (Figure 3a) while in γ-Mg-formate they are arranged in an orthogonal manner (Figure 3d). The μ^1 and μ^2 Mg−O bond distances in all three α, β and γ-Mg-formate range from 2.01 Å to 2.05 Å and 2.06 Å to 2.13 Å respectively.

Thermal Stability and PXRD Analysis. We have synthesized α- and γ-Mg-formates in bulk for in situ variable temperature PXRD analysis. To confirm the phase purity of the bulk materials, powder X-ray diffraction (PXRD) experiments were carried out on those compounds. The PXRD of experimental and computer-simulated pattern of γ-Mg-formate is shown in the Figure 4a. All major peaks of the experimental powder X-ray diffraction (PXRD) patterns match quite well that of simulated XRPD, indicating their reasonable crystalline phase purity. Thermal gravimetric analysis (TGA) performed on as-synthesized γ-Mg-formate revealed this compound's high thermal stability (see Section S3 in the Supporting Information for all data regarding guest mobility and thermal stability of γ-Mg-formate). The TGA trace for γ-Mg-formate showed a gradual weight-loss step of 27% (108−155 °C), corresponding to the escape of all solvent molecules trapped in the pores [$2(CH_3)_2NH$; calcd 27 %] followed by a plateau (155−370 °C) indicating its high thermal stability in the absence of guest molecules (Figure 4b). We note that the dimethylamine molecules in Mg-formate were released without damaging the frameworks, as evidenced by the coincidence of the PXRD patterns of the γ-Mg-formate powder sample heated to and held at 120 °C, in N_2 atmosphere with the PXRD patterns simulated from single crystal structures. Such high thermal and architectural stability of γ-Mg-formate was also verified from its in situ VT-PXRD patterns at different temperature which coincide with the patterns simulated from single crystal structures. In situ VT-PXRD of α-Mg-formate (Figure 4c) and γ-Mg-formate (Figure 4d) indicate the retention of crystallinity of these samples at high temperature. It also reveals that there are no possibilities of phase changes at higher temperature for these samples. We were unable to perform a VT-PXRD experiment on β-Mg-formate as all our attempts to synthesize it in phase pure bulk failed resulting in the production of a mixture of β-Mg-formate and anhydrous $Mg(HCOO)_2(HCOOH) \supset (CH_3)_2NH$.

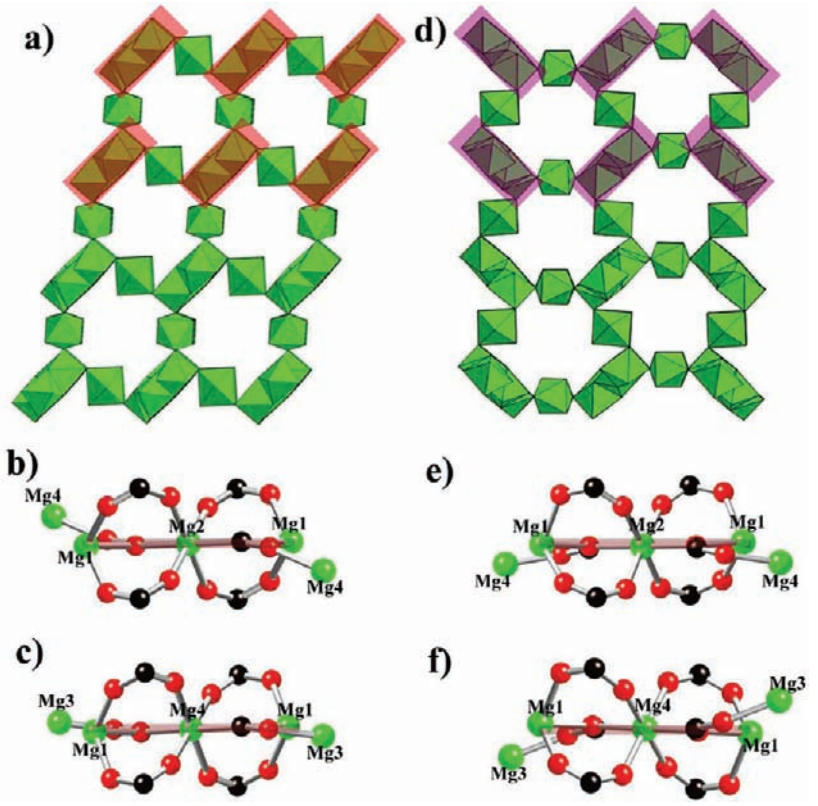

Figure 3. (a) Polyhedral representation of the extended structure of α-Mg-formate (parallel) viewed down the crystallographic *b* axis. (b) Trans orientation Mg(4) with respect to the planes formed by Mg(1)−Mg(2)−Mg(1). (c) Trans orientation Mg(3) with respect to the planes formed by Mg(1)−Mg(4)−Mg(1) in α-Mg-formate. (d) The polyhedral representation of the extended structure of γ-Mg-formate (orthogonal) viewed down the crystallographic *b* axis. (e) Cis orientation Mg(4) with respect to the planes formed by Mg(1)−Mg(2)−Mg(1). (f) Cis orientation Mg(3) with respect to the planes formed by Mg(1)−Mg(4)−Mg(1) in γ-Mg-formate.

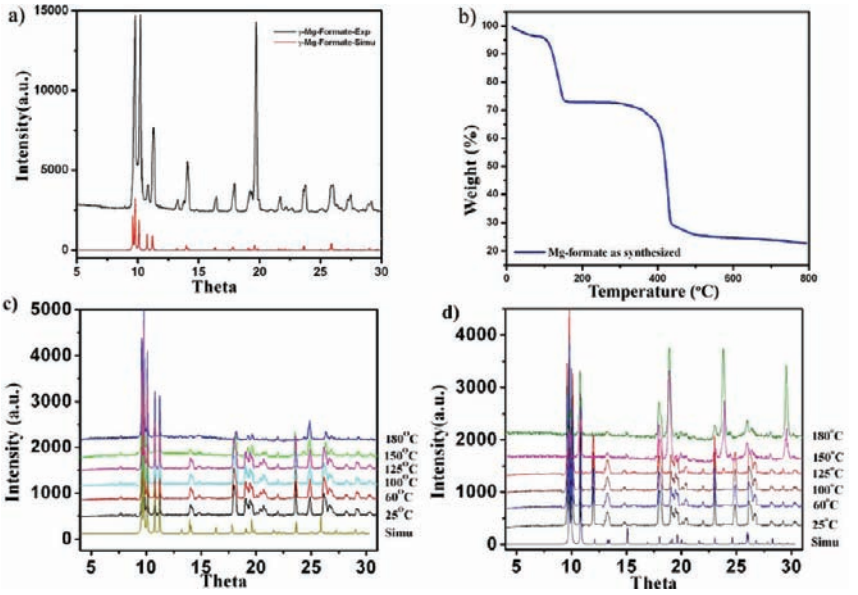

Figure 4. (a) Comparison of PXRD patterns of the as-synthesized γ-Mg-formate (black) with the simulated pattern from the single-crystal structure (red). (b) Thermogravimetric analysis of γ-Mg-formate (10 °C/min). (c) VT-PXRD patterns of γ-Mg-formate at different temperatures which coincides with the patterns simulated from single crystal structures. (d) VT-PXRD patterns of α-Mg-formate at different temperatures which coincides with the patterns simulated from single crystal structures.

Gas Adsorption Experiments. We focused to examine the porosity of γ-Mg-formate and prepared it at the gram scale to allow detailed investigation of the aforementioned property. An important structural feature of this γ-Mg-formate is that they possess pores (3.6 Å in diameter) (Figure 5a). Recently researchers envisaged that MOFs containing open Mg metal sites (Mg-MOF-74) rivals competitive materials in CO_2 capture, with 8.9 wt % dynamic capacity, and undergoes facile CO_2 release at 80 °C.[14] The dimethylamine molecules inside the pore in

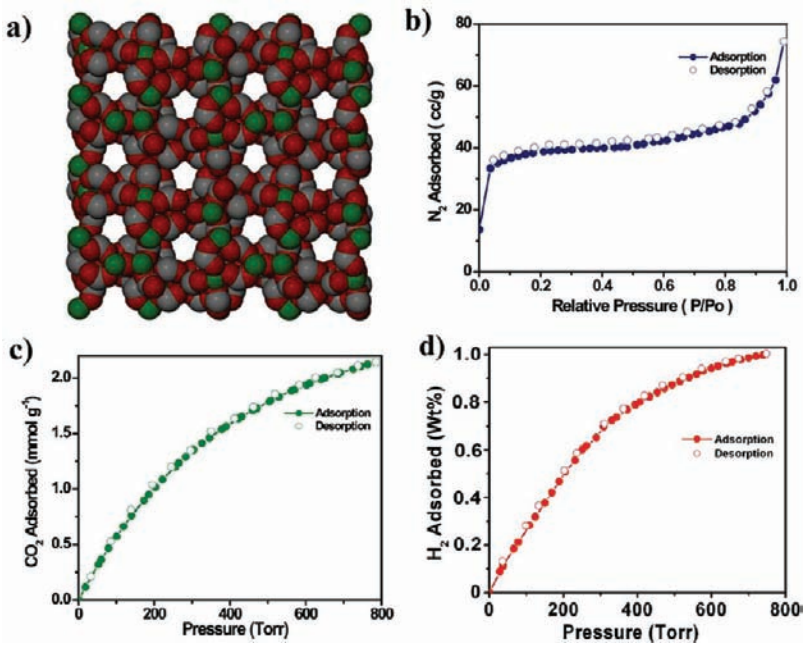

Figure 5. (a) Space fill model of γ-Mg-formate showing the 1D channels. Gas adsorption isotherms of γ-Mg-formate. (b) N_2 at 77 K (blue circles), (c) CO_2 (green circles), at 298 K, and (d) H_2 (red circles) at 77 K. The filled and open shapes represent adsorption and desorption, respectively. P/P_0, relative pressure at the saturation vapor pressure of the adsorbate gas.

as-synthesized γ-Mg-formate could be more readily removed by solvent-exchange. The thermogravimetric behavior of γ-Mg-formate was significantly simplified after they were immersed in organic solvents, such as chloroform. To remove the guest species from the frameworks and prepare the evacuated forms of γ-Mg-formate for gas-adsorption analysis, the as-synthesized γ-Mg-formate samples were immersed in chloroform at ambient temperature for 48 h, and evacuated at ambient temperature for 24 h, then at an elevated temperature (120 °C) for 6 h. The MOF sample thus obtained was optimally evacuated, as evident from the long plateau (108−370 °C) in the TGA traces.

The architectural rigidity and consequently the permanent porosity of evacuated γ-Mg-formate were unequivocally proven by gas-adsorption analysis. The nitrogen (N_2), hydrogen (H_2), and carbon-dioxide (CO_2) gas-adsorption experiments were carried out on γ-Mg-formate (Figure 5). These isotherms exhibit typical physisorption behavior, with a steep initial increase at low pressures and saturation at higher pressures. γ-Mg-formate adsorbs less nitrogen (38 cc gm^{-1}) than the α-Mg-formate (88 cc gm^{-1}) reported by Rood et al.[16b] As a result the specific surface area of γ-Mg-formate (Brunauer−Emmett−Teller (BET), 120 m^2 gm^{-1}) is lower than the α- polymorph (BET, 150 m^2 gm^{-1}). However, initial hydrogen uptake of γ-Mg-formate reached almost 1.0 wt % when the adsorbate pressure approached 760 Torr at 77 K (Figure 5b). This is higher than the hydrogen uptake of α-Mg-formate (0.6 wt %) reported by Rood et al.[16b] under similar conditions. It is noteworthy that low pressure hydrogen uptake of newly found γ-Mg-formate compares well with the reported hydrogen uptake of α-Mg-formate at pressure higher than 760 Torr.[16b] The maximum excess hydrogen uptake of the α-Mg-formate at 77 K is about 1.1 wt % with no hysteresis between adsorption and desorption. Although this H_2 adsorption is somewhat moderate, they compare well with the value of 0.7 wt % obtained for the highest capacity zeolite ZSM-5 and some of Mg-MOFs reported in the literature.[34] Recently researchers have shown that MOFs can hold large amounts of carbon dioxide and have demonstrated that MOFs can capture CO_2 selectively from CO and CH_4. Figure 6b shows the CO_2 adsorption isotherms for γ-Mg-formate, which shows a moderate affinity and capacity for CO_2 (3.4 Å kinetic diameter) at 298 K. The CO_2 uptake of γ-Mg-formate at 298 K (2.01 mmol gm^{-1}) (Figure 5c) is higher than the α-polymorph (1.69 mmol gm^{-1}). Although this CO_2 uptake is somewhat modest, but it compares well with the CO_2 uptake of several Mg-MOFs and ZIFs reported in the literature (see Table S2 and S3 in Supporting Information, for a detailed list of MOFs and Mg-MOFs with high CO_2 uptake).

Quantum Chemical Calculations. Portion of the 111 supercell of both α and γ-Mg-formate, which have been used for all ab initio quantum chemical calculation as cluster model (Supporting Information, Figure S8). It is clearly visible from the crystal structure of these two α and γ-Mg-formate (Figure 3) that there are highly electronegative oxygen atoms (from formate ligand), which are exposed to the pore surface. These particular surface areas have been scanned for adsorption energies and adsorption sites. We have calculated adsorption energies for each position for each hydrogen and compared the lowest energy positions at each surface sites. The adsorption energies we get are the local energy minima from every complete optimization cycle. Comparison of the adsorption energies often suggested similar adsorption energies and sites due to the choice of initial position of hydrogen molecules. The corresponding position of the hydrogen molecule with lowest adsorption energy can be obtained from the coordinate of the optimized geometry, which is depicted in Figure 6. It is clearly visible from Figure 6 that the hydrogen molecules are oriented toward

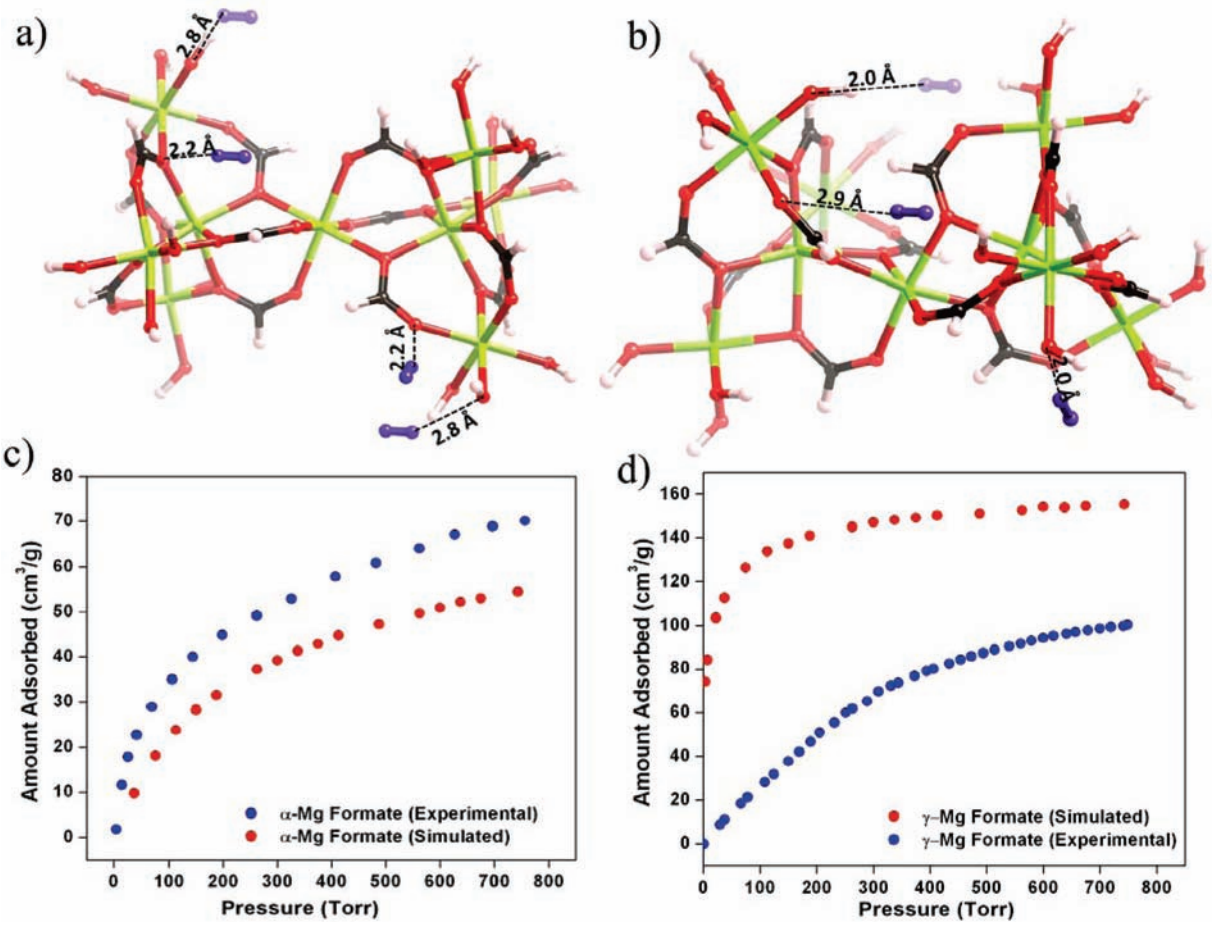

Figure 6. Different positions of hydrogen molecule in (a) α-Mg-formate cluster and (b) γ-Mg-formate cluster. Simulated and experimental isotherms for (c) α-Mg-formate and (d) γ-Mg-formate.

oxygen, that is, to the pore surface. This shows that oxygen atoms have pronounced affinity to bind to the free hydrogen molecules. The lowest energy adsorption sites of hydrogen molecules with respect to the oxygen atoms of formate anion are represented in Figure 6. The cluster for quantum chemical calculations was extracted from the supercells of these two formates. Therefore some oxygen carbon bonds were cleaved and hydrogen atoms saturated the dangling bonds. So the chemistry of those oxygen atoms changed, and we had two types of oxygen atoms in the cluster; the first one is the original formate oxygen from the supercell, and the second one is hydroxyl oxygen which we have generated while making the cluster (Figure 6a and 6b). We have found from this quantum chemical calculation that hydroxyl oxygen (binding energy is ~ -5.9 KJ/mol for α-formate and ~ -5.5 KJ/mol for γ-formate) has a higher affinity to attract hydrogen than the formate oxygen (~ -2.6 KJ/mol for both of them). But it is also evident that if we do not replace the formate oxygen with hydroxyl oxygen, a hydrogen molecule would interact with formate oxygen but with lesser interaction energy than that of hydroxyl oxygen.

Figures 6c and 6d shows the comparison between experimental and simulated single component H_2 adsorption isotherms of α-Mg-formate and γ-Mg-formate at the low pressure region. The excess amount adsorbed, N_{ex}, is defined as $N_{ex} = N_{total} - \rho V$, where ρ is the density of the bulk gas phase and V is the pore volume (calculated from the X-ray crystallographic structure). The data for the H_2 adsorption isotherm in α-Mg-formate has been taken from the literature.[16a] Calculated adsorption isotherms for pure H_2 are obtained by GCMC simulations. The GCMC simulations predict the measured and available experimental results with acceptable accuracy. The calculated loading of hydrogen in α-Mg-formate is 54.38 cc/g, and in the case of γ-Mg-formate the value is 155.34 cc/g at 760 Torr. pressure. The difference between experimental and simulated isotherms can be attributed to the contraction of pores after removal of the solvent.[35] These pore contractions of the γ-Mg-formate giving rise to lesser amount of loading with respect to the theoretically predicted isotherm which has been calculated from the original crystal structure (ignoring the solvent molecules). In addition, the empirical force fields used may not be accurate enough to describe such discrepancy, particularly in case of α-Mg-formate.

Conclusion

A new 3D magnesium formate polymorph, namely, γ-$[Mg_3(O_2CH)_6]$ has been synthesized via an in situ formate anion generation method and structurally characterized.

(35) The difference in the simulated and experimental adsorption isotherms could be due to poor activation as mentioned in the paper. However we cannot over rule the possibility of over estimation while calculating the simulated adsorption isotherm.

Crystal structure of this new γ polymorph of magnesium formate is completely different from other reported magnesium formates (α and β polymorph). The γ-Mg-formate has 1D channels along the *a*-axis, and shows reversible hydrogen ($\sim$1.0 wt % at 77 K, 760 Torr) and CO_2 uptake (2.1 mmol gm^{-1} at 298 K, 760 Torr). Quantum chemical calculation predicted the adsorption energies, which is in the range of physisorption and explains the low intake of hydrogen gas in this system. γ-Mg-formate outperforms the α and β polymorph with respect to CO_2 and H_2 uptake. This work may provide a potential way of using the in situ formate anion generation method for the design and synthesis of new MOFs. We, on the basis of the present work, are planning to investigate the possibility of preparing a series of metal formates to produce functionalized, porous, and lightweight framework materials.

Acknowledgment. A.M. and S.S. acknowledge CSIR, New Delhi, India for fellowship (JRF) support. P.P. acknowledges CSIR for a project assistantship (PA-II) from CSIR's XIth Five Year Plan Project (NWP0022-H). R.B. and S.R. acknowledge Dr. S. Sivaram, Director NCL for start-up grants and CSIR's XIth Five Year Plan Project (Grant NWP0022-H) for funding and also Dr. S. Pal and Dr. K. Vijaymohanan for their encouragement. S.R. acknowledges the Center for Scientific Computing at NCL for providing computing time for the project Financial assistance from the DST (SR/S1/IC-22/2009) is acknowledged.

Supporting Information Available: Description of experimental details, including synthetic methods, crystallography, supplementary figures, including TGA, infrared spectroscopy, powder XRD profile, table of crystallographic data and CIF file, and anisotropic thermal ellipsoids for γ-Mg-formate reported in this paper. This material is available free of charge via the Internet at http://pubs.acs.org.